Article

Understanding Binding Affinity: A Combined Isothermal Titration Calorimetry/Molecular Dynamics Study of the Binding of a Series of Hydrophobically Modified Benzamidinium Chloride Inhibitors to Trypsin

Reinskje Talhout, Alessandra Villa, Alan E. Mark, and Jan B. F. N. Engberts

J. Am. Chem. Soc., **2003**, 125 (35), 10570-10579• DOI: 10.1021/ja034676g • Publication Date (Web): 09 August 2003

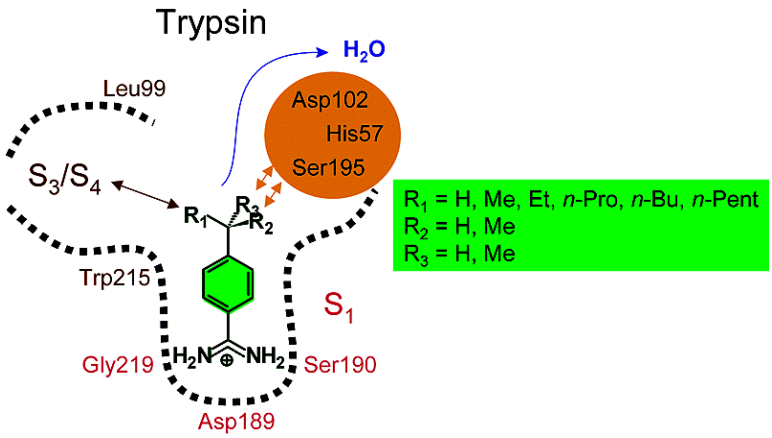

More About This Article

Additional resources and features associated with this article are available within the HTML version:

- Supporting Information
- Links to the 5 articles that cite this article, as of the time of this article download
- Access to high resolution figures
- Links to articles and content related to this article
- Copyright permission to reproduce figures and/or text from this article

View the Full Text HTML

J|A|C|S
ARTICLES
Published on Web 08/09/2003

Understanding Binding Affinity: A Combined Isothermal Titration Calorimetry/Molecular Dynamics Study of the Binding of a Series of Hydrophobically Modified Benzamidinium Chloride Inhibitors to Trypsin

Reinskje Talhout,[†] Alessandra Villa,[‡] Alan E. Mark,[‡] and Jan B. F. N. Engberts*,[†]

Contribution from the Physical Organic Chemistry Unit, Stratingh Institute, University of Groningen, and the Groningen Biomolecular Sciences and Biotechnology Institute, Department of Biophysical Chemistry, University of Groningen, Nijenborgh 4, 9747 AG Groningen, The Netherlands

Received February 14, 2003; E-mail: J.B.F.N.Engberts@chem.rug.nl

Abstract: The binding of a series of *p*-alkylbenzamidinium chloride inhibitors to the serine proteinase trypsin over a range of temperatures has been studied using isothermal titration (micro)calorimetry and molecular dynamics simulation techniques. The inhibitors have small structural variations at the para position of the benzamidinium ion. They show small differences in relative binding affinity but large compensating differences in enthalpy and entropy. Binding affinity decreases with increased branching at the first carbon but increases with increasing the length of a linear alkyl substituent, suggesting that steric hindrance and hydrophobic interactions play dominant roles in binding. Structural analysis showed that the backbone of the enzyme was unaffected by the change of the para substituent. In addition, binding does not correlate strongly with octanol/water partition data. To further characterize this system, the change in the heat capacity on binding, the change in solvent-accessible surface area on binding, the effect of inhibitor binding on the hydration of the active site, the pK_a of His57, and interactions within the catalytic triad have been investigated. Although the changes in inhibitor structure are small, it is demonstrated that simple concepts such as steric hindrance, hydrophobicity, and buried surface area are insufficient to explain the binding data. Other factors, such as access to the binding site and the cost of dehydration of the active site, are of equal or greater importance.

Introduction

Knowledge of the factors that determine the binding affinity of low-molecular-weight compounds to proteins is of fundamental scientific interest as well as a prerequisite for structure-based drug design.[1,2] One approach to evaluate the contribution of a specific part of the inhibitor is to study the influence of small structural variations on the thermodynamics of binding.[3−5] Here we present a combined structural and thermodynamic study of the binding of *p*-alkylbenzamidinium chloride inhibitors to the serine proteinase trypsin. Serine proteinases are important targets for medicinal chemistry that are associated with a wide range of biologically important processes, including digestion (trypsin, elastase), blood coagulation (thrombin, factor Xa), and fertilization (plasmin).[6,7] They are specific for arginine or lysine, and many natural peptide inhibitors have an arginine or lysine that binds in the specificity pocket. Synthetic inhibitors are often based on analogous groups.[8] In particular, benzamidinium, a structural mimic of arginine and itself a potent inhibitor,[9] is the primary component of many larger inhibitors.[4,10,11] The structures of benzamidinium, and a wide range of benzamidinium derivatives, complexed with trypsin are known.[12,13]

Figure 1 shows the benzamidinium ion bound in the pocket S1 of trypsin, hydrogen-bonded to Asp189, Gly219, Ser190, and an internal water molecule. In other systems, water molecules have been shown to complement the interaction between a ligand and a receptor. The net thermodynamic effect of such water molecules, however, varies.[2] Benzamidinium

[†] Physical Organic Chemistry Unit, Stratingh Institute.
[‡] Groningen Biomolecular Sciences and Biotechnology Institute (GBB), Department of Biophysical Chemistry.

(1) Böhm, H.-J.; Klebe, G. *Angew. Chem., Int. Ed. Engl.* **1996**, *35*, 2588−2614.
(2) *Structure-Based Drug Design: Thermodynamics, Modeling and Strategy*; Ladbury, J. E., Connelly, P. R., Eds.; Springer: Berlin, 1997.
(3) Fersht, A. *Structure and Mechanism in Protein Science*; Freeman: New York, 1999.
(4) Dullweber, F.; Stubbs, M. T.; Musil, D.; Stürzebecher, J.; Klebe, G. *J. Mol. Biol.* **2001**, *313*, 593−614.
(5) Morgan, B. P.; Scholtz, J. M.; Ballinger, M. D.; Zipkin, I. D.; Bartlett, P. A. *J. Am. Chem. Soc.* **1991**, *113*, 297−307.
(6) *Proteases, Potential Role in Health and Disease*; Hörl, W. H., Heidland, A., Eds.; Plenum Press: New York, 1984.
(7) *Proteinases in Mammalian Cells and Tissues*; Barrett, A. J., Ed.; Elsevier: Amsterdam, 1977.
(8) *Proteinase Inhibitors*; Barrett, A. J., Salvesen, G., Eds.; Elsevier: Amsterdam, 1986.
(9) Mares-Guia, M.; Shaw, E. *J. Biol. Chem.* **1965**, *240*, 1579−1585.
(10) Bohm, M.; Stürzebecher, J.; Klebe, G. *J. Med. Chem.* **1999**, *42*, 458−477.
(11) Renatus, M.; Bode, W.; Huber, R.; Stürzebecher, J.; Stubbs, M. T. *J. Med. Chem.* **1998**, *41*, 5445−5456.
(12) Marquart, M.; Walter, J.; Deisenhofer, J.; Bode, W.; Huber, R. *Acta Crystallogr.* **1983**, *B39*, 480−490.
(13) Bode, W.; Schwager, P. *J. Mol. Biol.* **1975**, *98*, 693−717.

10.1021/ja034676g CCC: $25.00

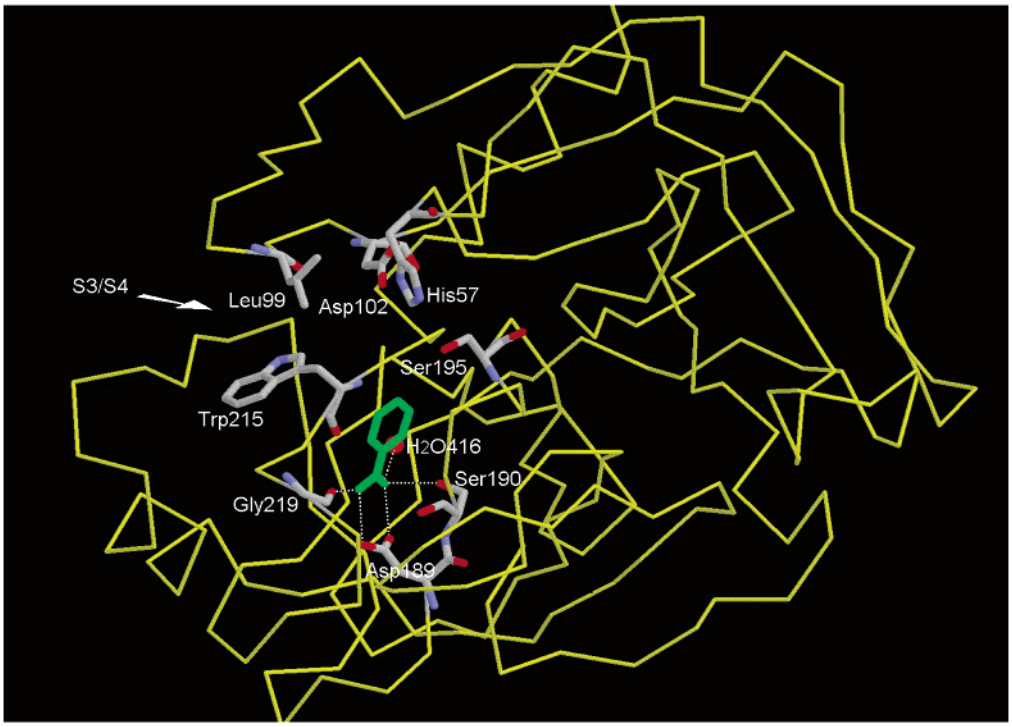

Figure 1. Backbone representation of the benzamidinium−trypsin complex[12] (3PTB from the Protein Data Bank) generated using RasMol.[14] Benzamidinium (green) is bound in the S1 binding pocket, close to residues of the catalytic triad, His57 and Ser195. The phenyl ring of the benzamidinium is in van der Waals contact with residues 214−216 and 190−191. Also shown is the hydrophobic pocket S3/S4, defined by Trp215 and Leu99.

Chart 1. Structures of the *p*-Alkylbenzamidinium Chlorides Studied[a]

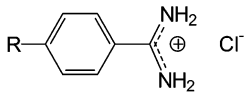

[a] R = Me, Et, *n*-Pr, *i*-Pr, *n*-Bu, *t*-Bu, *n*-Pent, *n*-Hex.

derivatives containing large hydrophobic groups often also occupy the hydrophobic S3/S4 groove, defined by the residues Trp215 and Leu99.[4,11]

There have been many studies of the binding of benzamidinium derivatives to trypsin. Often, however, only the binding constant has been considered, potentially leading to the (erroneous) conclusion that some structural variations do not affect binding significantly. Also, the structural variations are often large, which makes it difficult to infer the precise reason for changes in binding affinity. In this work we consider the effect of small systematic changes to the para substituent of benzamidinium on the thermodynamics of binding to trypsin. Previously,[15] we showed that the electronic properties of a substituent strongly affect binding. Here we consider the role that steric and hydrophobic effects play in determining the interaction with the enzyme.

To systematically probe the role of steric and hydrophobic effects in binding, we have studied a series of *p*-alkyl-substituted benzamidinium chlorides (Chart 1) by means of isothermal titration calorimetry (ITC) and molecular dynamics (MD) simulation techniques. The substituents differ in the degree of branching at the first carbon atom and the length of the carbon chain. Their electronic properties are, however, very similar, with Hammett substituent constants (σ_p^+)[16] ranging between −0.31 and −0.26. Any significant differences in binding affinities of the inhibitors cannot be attributed to inductive or resonance effects of the substituents.

To quantify the effect of varying the substituent, ITC was used to acquire a complete thermodynamic description of binding. The advantage of ITC over kinetic techniques is that it is efficient and noninvasive.[17−19] One experiment provides the binding constant and the enthalpy of binding, from which the Gibbs energy and entropy of binding are readily calculated. The enthalpic and entropic contributions to the Gibbs energy of binding were used to infer information regarding the mechanism of binding. While small structural variations in an inhibitor often result in only small changes in the Gibbs energy of binding, the enthalpy and entropy may vary considerably. Such enthalpy−entropy compensation is common when studying weak interactions and is important for understanding the nature of competing interactions.[20−22] The temperature dependence of the enthalpy of binding also gives valuable information on the origin of the interaction.[2]

The enthalpy of binding, the entropy of binding, and the Gibbs energy are, however, global properties of the system. They can neither be used to infer the precise nature of an interaction, nor to provide a detailed structural model. MD computer simulations have, therefore, been used to link the experimentally measured

(14) Rasmol 2.7.2; Herbert J. Bernstein, August 2000.
(15) Talhout, R.; Engberts, J. B. F. N. *Eur. J. Biochem.* **2001**, *268*, 1554−1560.
(16) Exner, O. The Hammett Equation−The Present Position. In *Advances in Linear Free Energy Relationships*; Chapman, N. B., Shorter, J., Eds.; Plenum Press: London, 1972; pp 1−69.
(17) Holdgate, G. A. *Biotechniques* **2001**, *30*, 164−184.
(18) Leavitt, S.; Freire, E. *Curr. Opin. Struct. Biol.* **2001**, *11*, 560−566.
(19) *Applications of Calorimetry in the Biological Sciences*; Ladbury, J. E., Chowdry, B. Z., Eds.; Wiley: New York, 1998.
(20) Calderone, C. T.; Williams, D. H. *J. Am. Chem. Soc.* **2001**, *123*, 6262−6267.
(21) Cooper, A.; Johnson, C. M.; Lakey, J. H.; Nöllmann, M. *Biophys. Chem.* **2001**, *93*, 215−230.
(22) Dunitz, J. D. *Chem. Biol.* **1995**, *2*, 709−712.

thermodynamic properties to the microscopic structure of the system. Specifically, MD simulations have been used to study the structural changes that accompany binding and to predict the change in Gibbs energy given a particular structural model.

Experimental Section

Synthesis of Inhibitors. The *p*-alkylbenzamidinium chlorides were synthesized using modified literature procedures.[23−25] Details of the synthesis and analysis of the products are given in the Supporting Information.

Isothermal Titration Calorimetry. Trypsin solutions were prepared as described previously.[15] Titration experiments were performed using either an Omega isothermal titration calorimeter (Microcal, Inc., Northampton, MA) coupled to a nanovolt preamplifier in order to improve the signal-to-noise ratio or an MCS isothermal titration calorimeter (Microcal, Inc.). Both machines were connected to a water bath for temperature control. The instruments were calibrated using standard electrical pulses. Inhibitor solutions (5−10 mM, determined by weight, depending on the specific inhibitor) were titrated into the stirred (350 rpm) cell (1.3249 or 1.3496 mL, respectively) containing a degassed (ca. 10 min) trypsin solution (ca. 0.15 mM) after a stable baseline (rms noise < 0.0050) was achieved. The injection sequence consisted of an initial injection of 1 μL to prevent artifacts arising from the filling of the syringe (not used in data fitting), followed by injections of 5 μL each at 300-s intervals until saturation was reached. To correct for the heat of dilution and mixing, blank titrations of inhibitor into buffer were subtracted from the inhibitor−enzyme titration. Data were analyzed using Origin software (Microcal, Inc.), assuming a single binding site.[26] This yielded ΔH (enthalpy of binding) and K (binding constant). Measurements were repeated at least three times; K was reproducible to within 10%, and ΔH was reproducible to within 5%. Errors in ΔC_p were within 5%.

Computational Techniques. The starting structure of the benzamidinium−trypsin complex was taken from the Brookhaven Protein Data Bank (PDB structure 3PTB).[12] The nine inhibitors were placed in the S1 pocket of the enzyme by superimposing the benzamidinium ion within the crystallographic complex. The protein and the bound inhibitor were hydrated in a box containing ∼5700 simple point charge (SPC)[27] water molecules. The protein and inhibitors were described using the GROMOS96 (43a2) force field,[28,29] in which aliphatic hydrogen atoms are treated as united atoms, together with the carbon atom to which they are attached. The charges of ionizable groups were appropriate for pH 7.0. Arg and Lys were protonated. Asp and Glu were unprotonated. Histidines were neutral. Tautomeric forms were based on local interactions. For His57, which is close to the binding pocket, the Nδ_1−H tautomer was chosen.

All simulations were performed using the GROMACS (version 3.0) package[30−32] in a periodic triclinic box. Nonbonded interactions were evaluated using a twin range cutoff. Interactions within the shorter-range cutoff (0.9 nm) were evaluated every step, whereas interactions within the longer cutoff (1.4 nm) were updated every five steps, together with the pair list. To correct for the neglect of electrostatic interactions beyond the 1.4 nm cutoff, a reaction field (RF) correction with $\epsilon_{RF} = 78.0$ was used. To maintain constant temperature and pressure, a Berendsen thermostat[33] was applied. The protein, inhibitor, and solvent were independently coupled to a temperature bath (25 °C) with a coupling time of 0.1 ps. The pressure was held at 1 bar, with a coupling time of 0.5 ps. The isothermal compressibility was 4.6×10^{-5} bar^{-1}.[33] The time step was 0.002 ps. The bond lengths and angle in water were constrained using the SETTLE algorithm.[34] Bond lengths within the protein were constrained using the LINCS algorithm.[35]

Free Energy Calculations. The difference in Gibbs energy between two states of a system was determined using the coupling parameter approach in conjunction with the thermodynamic integration (TI) formula:[36]

$$\Delta G_{A-B} = \int_{\lambda_A}^{\lambda_B} \left\langle \frac{\partial H(\lambda)}{\partial \lambda} \right\rangle_\lambda d\lambda \quad (1)$$

In this approach, the Hamiltonian H is made a function of a coupling parameter, λ. The λ-dependence of the Hamiltonian defines a pathway which connects two states of the system, denoted by A and B. To solve eq 1, the ensemble average at a number of discrete λ-points was obtained by performing separate simulations for each chosen λ-point, and the integral was determined numerically.

The change in Gibbs energy resulting from the changes in the inhibitor (or protein) was achieved by gradually mutating the atoms of state A into the atoms of state B. Atoms with no corresponding atoms in the other state were mutated to "dummy" atoms. A dummy atom has no nonbonded (Lennard-Jones or electrostatic) interactions with other atoms. The mutations in this study involved only nonbonded interactions. The bonded interactions and the masses of the atoms were not changed, as they make no net contribution to the change in binding Gibbs energy. The nonbonded interactions between the initial state (A) and the final state (B) were interpolated using a soft-core potential,[37] as implemented in the GROMACS simulation package.[31,38]

Separate simulations were performed at 18 λ-points from $\lambda = 0$ (state A) to $\lambda = 1$ (state B). At each λ-point, the system was equilibrated for 50 ps and data were collected for 150 (free inhibitor) or 250 ps (complex). For complexes with alkyl chains longer than *n*-propyl, 22 λ points were used with 500 ps sampling. To obtain ΔG_{A-B}, the average, $\langle \partial H(\lambda)/\partial\lambda \rangle_\lambda$, at each λ-point (eq 1) was integrated using the trapezoidal method. The error in $\langle \partial H(\lambda)/\partial\lambda \rangle_\lambda$ was estimated using a block averaging procedure,[39,40] and the errors were integrated to give the total error in ΔG_{A-B}.

Results and Discussion

Binding Affinity. The thermodynamics of binding of *p*-alkylbenzamidinium chlorides (Chart 1) to trypsin were studied using ITC. Since the solubility of *p*-*n*-hexylbenzamidinium chloride (∼15 mM) was only 3 times higher than the concentration necessary for the experiments (∼5 mM), solubility problems

(23) Glock, G. *Chem. Ber.* **1888**, *21*, 2650−2659.
(24) Rash, F. H.; Boatman, S.; Hauser, C. R. *J. Org. Chem.* **1967**, *32*, 372−376.
(25) Moss, R. A.; Ma, W.; Merrer, D. C.; Xue, S. *Tetrahedron Lett.* **1995**, *36*, 8761−8764.
(26) Wiseman, T.; Williston, S.; Brandts, J. F.; Lin, L. N. *Anal. Biochem.* **1989**, *179*, 131−137.
(27) Berendsen, H. J. C.; Postma, J. P. M.; van Gunsteren, W. F.; Hermans, J. In *Intermolecular Forces*; Pullman, B., Ed.; Reidel: Dordrecht, 1981; pp 331−342.
(28) van Gunsteren, W. F.; Billeter, S. R.; Eising, A. A.; Hünenberger, P. H.; Krüger, P.; Mark, A. E.; Scott, W. R. P.; Tironi, I. G. *Biomolecular Simulation: GROMOS96 Manual and User Guide*; BIOMOS b.v.: Zürich, Groningen, 1996.
(29) Schuler, L. D.; van Gunsteren, W. F. *Mol. Sim.* **2000**, *25*, 301−319.
(30) Berendsen, H. J. C.; van der Spoel, D.; van Drunen, R. *Comput. Phys. Commun.* **1995**, *91*, 43−56.
(31) Lindahl, E.; Hess, B.; van der Spoel, D. *J. Mol. Model.* **2001**, *7*, 306−317.
(32) van der Spoel, D.; van Buuren, A. R.; Apol, E.; Meulenhoff, P. J.; Tieleman, D. P.; Sijbers, A. L. T. M.; Hess, B.; Feenstra, K. A.; Lindahl, E.; van Drunen, R.; Berendsen, H. J. C. *Gromacs User Manual Version 3.0*; Nijenborgh 4, 9747 AG Groningen, The Netherlands, 2001 (http://www.gromacs.org).
(33) Berendsen, H. J. C.; Postma, J. P. M.; van Gunsteren, W. F.; DiNola, A.; Haak, J. R. *J. Chem. Phys.* **1984**, *81*, 3684−3690.
(34) Miyamoto, S.; Kollman, P. A. *J. Comput. Chem.* **1992**, *13*, 952−962.
(35) Hess, B.; Bekker, H.; Berendsen, H. J. C.; Fraaije, J. G. E. M. *J. Comput. Chem.* **1997**, *18*, 1463−1472.
(36) Mark, A. E. In *Encyclopedia of Computational Chemistry*; von Ragué Schleyer, P., Ed.; Wiley: New York, 1998; pp 1070−1083.
(37) Beutler, T. C.; Mark, A. E.; van Schaik, R. C.; Geber, P. R.; van Gunsteren, W. F. *Chem. Phys. Lett.* **1994**, *222*, 529−539.
(38) Villa, A.; Mark, A. E. *J. Comput. Chem.* **2002**, *23*, 548−553.
(39) Bishop, M.; Frinks, S. *J. Chem. Phys.* **1987**, *87*, 3675−3676.
(40) Allen, M. P.; Tildesley, D. J. *Computer Simulations of Liquids*; Oxford Science Publications: Oxford, 1987.

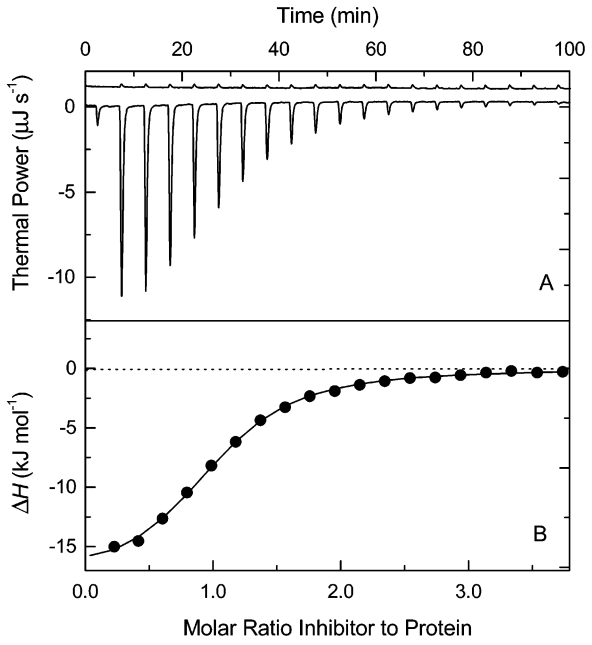

Figure 2. (A) Raw data for titration of *p*-methylbenzamidinium chloride into an aqueous trypsin (lower trace) and buffer (upper trace) solution at 25 °C in Tris at pH 8.0. (B) Enthalpogram retrieved from (A), corrected for the heat of dilution; the line represents the least-squares fit to the single-site binding model.[26]

are anticipated for alkyl chains longer than *n*-hexyl. No attempt was made to study longer chain *p*-*n*-alkylbenzamidinium chlorides.

Figure 2A shows the raw data of a typical binding experiment, the titration of *p*-methylbenzamidinium chloride to trypsin in Tris buffer at 25 °C. Binding is strongly exothermic. Note that the dilution peaks are small, endothermic, and equal in size. This indicates that, at this concentration, no aggregation of the inhibitor in water occurs. Figure 2B shows the corresponding enthalpogram. Similar observations were made for all other inhibitors. A binding isotherm (see Experimental Section) has been fitted to the data to obtain values for K and ΔH. From these values, ΔG and $T\Delta S$ can be calculated using

$$\Delta G = -RT \ln K = \Delta H - T\Delta S \qquad (2)$$

Titration experiments were performed at 20, 25, 30, and 37 °C in Tris buffer. The resulting thermodynamic parameters are listed in Table 1. Benzamidinium chloride is also listed for comparison but is not considered a member of this series due to different electronic para-substituent effects. Changes in the alkyl substituent at the para position lead to systematic differences in binding affinities (Table 1). At all temperatures studied, *p*-*n*-hexylbenzamidinium chloride (the best inhibitor) binds ~14 times more tightly than *p*-isopropylbenzamidinium chloride (the worst).

In Figure 3, the change in Gibbs energy ($\Delta\Delta G$) at 25 °C relative to *p*-methylbenzamidinium is plotted. Figure 3A shows the effect of increasing the branching at the first position of the chain, and Figure 3B shows the effect of increasing the length of the chain. This relative order of binding was found for all temperatures studied, except for a reversal of *n*-Pent and H at 20 °C and *n*-Pent and Me at 37 °C.

The structure and dynamics of the complexes were also investigated using MD simulations. Each complex was simulated

Table 1. Thermodynamic Parameters of Binding of *p*-Alkylbenzamidinium Chlorides to Trypsin at Several Temperatures[a]

R[b]	T (°C)	K (10^4 M^{-1})	ΔG (kJ mol^{-1})	ΔH (kJ mol^{-1})	$T\Delta S$ (kJ mol^{-1})
H[c]	20.1	6.2 ± 0.5	−26.9 ± 0.2	−17.0 ± 0.4	9.9 ± 0.5
	25.1	4.5 ± 0.2	−26.6 ± 0.3	−18.9 ± 0.4	7.7 ± 0.6
	30.0	4.1 ± 0.3	−26.7 ± 0.2	−21.4 ± 1.0	5.4 ± 0.5
	37.1	3.1 ± 0.3	−26.7 ± 0.3	−23.7 ± 1.2	3.0 ± 0.7
Me[c]	20.1	8.0 ± 0.7	−27.5 ± 0.3	−16.7 ± 0.4	10.8 ± 0.6
	25.1	6.9 ± 0.3	−27.6 ± 0.1	−18.5 ± 0.3	9.1 ± 0.2
	30.0	5.5 ± 0.2	−27.5 ± 0.2	−20.7 ± 0.3	6.8 ± 0.3
	37.1	4.1 ± 0.4	−27.4 ± 0.2	−23.8 ± 0.6	3.6 ± 0.5
Et[d]	20.0	3.4 ± 0.1	−25.5 ± 0.1	−10.6 ± 0.2	14.9 ± 0.4
	25.1	2.9 ± 0.2	−25.4 ± 0.2	−13.9 ± 0.6	11.5 ± 0.7
	30.0	2.5 ± 0.2	−25.5 ± 0.2	−17.3 ± 0.5	8.2 ± 0.6
	37.1	2.1 ± 0.3	−25.6 ± 0.3	−22.4 ± 0.8	3.2 ± 0.5
n-Pr	20.1	3.8 ± 0.3	−25.7 ± 0.2	−9.7 ± 0.4	16.0 ± 0.5
	25.2	3.1 ± 0.2	−25.7 ± 0.2	−12.7 ± 0.5	13.0 ± 0.6
	30.2	2.5 ± 0.1	−25.6 ± 0.1	−15.7 ± 0.6	9.9 ± 0.4
	37.2	2.0 ± 0.2	−25.6 ± 0.3	−19.9 ± 0.7	5.7 ± 0.8
i-Pr[d]	20.0	1.1 ± 0.08	−22.6 ± 0.2	−4.9 ± 0.2	18 ± 0.4
	25.0	0.96 ± 0.09	−22.7 ± 0.2	−7.0 ± 0.4	16 ± 0.5
	30.0	0.84 ± 0.07	−22.8 ± 0.2	−9.0 ± 0.4	14 ± 0.6
	37.0	0.66 ± 0.05	−22.7 ± 0.2	−12 ± 0.5	11 ± 0.5
n-Bu	20.0	4.7 ± 0.3	−26.2 ± 0.3	−6.1 ± 0.3	20.1 ± 0.5
	25.1	3.8 ± 0.2	−26.2 ± 0.2	−9.9 ± 0.5	16.3 ± 0.7
	30.0	3.4 ± 0.2	−26.3 ± 0.2	−13.4 ± 0.6	12.9 ± 0.7
	37.0	2.7 ± 0.1	−26.3 ± 0.2	−18.5 ± 0.9	7.8 ± 0.6
t-Bu[e]		-	-	-	-
n-Pent	20.0	6.0 ± 0.5	−26.8 ± 0.2	−6.6 ± 0.3	20.3 ± 0.6
	25.0	5.8 ± 0.3	−27.2 ± 0.1	−9.9 ± 0.4	17.3 ± 0.3
	30.0	5.3 ± 0.5	−27.4 ± 0.2	−12.8 ± 0.6	14.6 ± 0.7
	37.0	5.0 ± 0.4	−27.9 ± 0.2	−17.5 ± 0.8	10.4 ± 0.7
n-Hex	20.0	14 ± 1	−28.9 ± 0.2	−6.6 ± 0.2	22.2 ± 0.2
	25.0	13 ± 0.6	−29.2 ± 0.1	−10.6 ± 0.2	18.6 ± 0.3
	30.0	12 ± 0.7	−29.4 ± 0.2	−15.1 ± 0.4	14.3 ± 0.2
	37.0	10 ± 0.6	−29.7 ± 0.2	−21.0 ± 0.6	8.7 ± 0.5

[a] Titrations performed in 50 mM Tris, 10 mM $CaCl_2$ buffer at pH 8.0. [b] Substituent at para position. [c] Data taken from ref 15. [d] Since these compounds contain some NH_4Cl, control experiments were performed with 10 wt % NH_4Cl added to a benzamidinium chloride solution at the usual concentration. Within error, the thermodynamic parameters were identical. Therefore, the concentration of these inhibitors, based on weight, can be safely corrected for the amount of NH_4Cl present. [e] When *p*-*tert*-butylbenzamidinium chloride was titrated into trypsin, only peaks of dilution were observed at 25 °C. Therefore, binding of this compound is negligible, and it is therefore not considered an inhibitor.

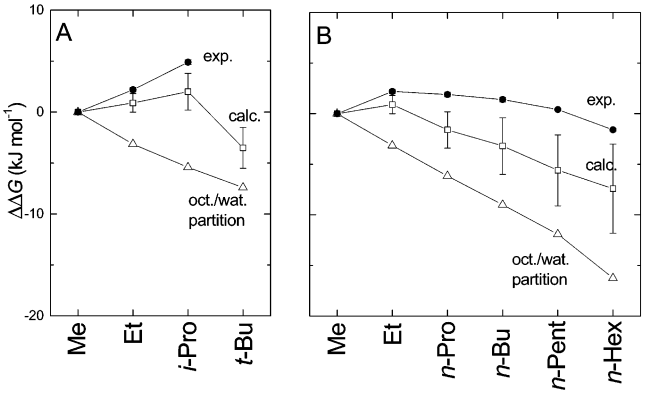

Figure 3. Experimental (●) and calculated (□) relative Gibbs energies of binding to trypsin of *p*-alkylbenzamidinium ions with respect to the *p*-methylbenzamidinium ion at 25 °C. The difference in Gibbs energy of octanol/water partitioning[41] (△) is also reported. (A) Values for the methyl-, ethyl-, isopropyl-, and *tert*-butylbenzamidinium ions, showing the effect of branching at the first carbon. (B) Values for the methyl-, ethyl-, *n*-propyl-, *n*-butyl-, *n*-pentyl-, and *n*-hexylbenzamidinium ions, showing the effect of extending the aliphatic chain.

for at least 15 ns (5 ns equilibration, 10 ns sampling). For alkyl chains longer than *n*-propyl, the simulations were 25 ns (5 ns equilibration; 20 ns sampling). In all cases, the structures

Table 2. RMS Positional Deviations (nm)[a] of the Backbone Atoms, the Backbone Atoms within 1.4 nm of the Inhibitor, the Phenyl Ring, and Some Residues with Respect to the Crystallographic Structure for the *p*-Alkylbenzamidinium−Trypsin Complexes Studied

R[b]	backbone	backbone (1.4 nm)	phenyl ring	Asp189, Ser190, Gly219
H	0.14	0.12	0.15	0.13
Me	0.17	0.14	0.10	0.11
Et	0.13	0.12	0.08	0.11
n-Pr	0.20	0.17	0.01	0.18
i-Pr	0.15	0.11	0.11	0.17
n-Bu	0.15	0.12	0.09	0.12
t-Bu	0.14	0.12	0.13	0.16
n-Pent	0.18	0.14	0.11	0.11
n-Hex	0.16	0.13	0.11	0.15

[a] The RMS deviations were calculated for each frame after a least-squares fit on the backbone. [b] Substituent at para position.

remained close to that of the benzamidinium-trypsin complex[12] on which the starting configurations were based. Table 2 shows the average root-mean-square (RMS) deviation of the complexes with respect to the crystal structure 3PTB. The RMS deviation was evaluated after performing a least-squares best fit on all backbone atoms. The RMS deviations of the backbone atoms with respect to the X-ray structure were between 0.13 and 0.20 nm (Table 2). The position of the phenyl ring of the inhibitor was the same as that observed in the crystal structure 3PTB for all compounds. No obvious strain is present in any of the structures.

For comparison to the ITC results, the relative Gibbs energies of binding of the inhibitors to trypsin at 25 °C were calculated. The relative binding Gibbs energy ($\Delta\Delta G_{A\rightarrow B}$) of inhibitor B with respect to inhibitor A was evaluated using the following thermodynamic cycle:

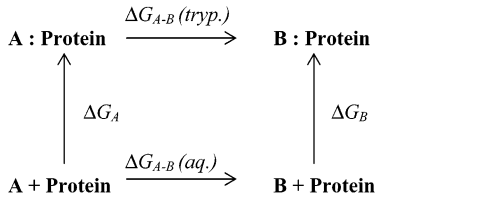

$$\Delta\Delta G_{A\rightarrow B} = \Delta G_B - \Delta G_A = \Delta G_{A-B}(tryp.) - \Delta G_{A-B}(aq.) \quad (3)$$

where ΔG_A and ΔG_B are the binding Gibbs energy of inhibitor A and B, respectively, and ΔG_{A-B} is the work required to mutate inhibitor A into B in trypsin (ΔG_{A-B}(tryp.)) and in water (ΔG_{A-B}(aq.)). As the Gibbs energy is a state function, the change in Gibbs energy for any closed cycle is zero. Thus, the difference $\Delta\Delta G_{A\rightarrow B}$ may be obtained either by calculating ΔG_A and ΔG_B, which corresponds to simulating the process of complexation, or by the computationally more efficient approach of determining ΔG_{A-B}(tryp.) and ΔG_{A-B}(aq.). This corresponds to the (nonphysical) mutation of A into B in the complex and free in solution. The change in binding Gibbs energy was estimated using the TI formula (see Experimental Section). In Table 3, the experimental and calculated relative binding Gibbs energies at 25 °C are reported for all the transformations investigated.

The estimates from the free energy calculations of the changes in Gibbs energy relative to *p*-methylbenzamidinium are shown in Figure 3, along with the experimental results. Overall, relative

Table 3. Experimental and Calculated Relative Binding Gibbs Energies, $\Delta\Delta G_{A\rightarrow B}$, at 25 °C for All Mutations Investigated

mutation $R_A \rightarrow R_B$	$\Delta\Delta G_{A\rightarrow B}$ (kJ mol^{-1}) exptl	calcd
H → Me	−1.0 ± 0.2	−1.3 ± 0.8
Me → Et	2.1 ± 0.1	0.9 ± 0.9
Et → *n*-Pr	−0.3 ± 0.3	−2.5 ± 0.9
n-Pr → *n*-Bu	−0.5 ± 0.3	−1.6 ± 1.0
n-Bu → *n*-Pent	−1.0 ± 0.1	−2.4 ± 0.7
n-Pent → *n*-Hex	−2.0 ± 0.1	−1.8 ± 0.9
Et → *i*-Pr	2.7 ± 0.3	1.1 ± 0.9
Et → *t*-Bu		−4.4 ± 1.1

Gibbs energies of binding calculated from the simulations show good agreement with the experimental trends. The exception is *tert*-butylbenzamidinium, which was predicted to have a binding constant similar to that of *n*-butylbenzamidinium but did not bind in ITC experiments. Note that, in the simulations, the inhibitor is grown directly inside the S1 pocket. If the *tert*-butyl inhibitor were unable to enter the S1 pocket, this would not be reflected in the calculations. To test if the binding of *tert*-butylbenzamidinium was on a time scale not detectable using the standard ITC approach, a competitive binding experiment was also performed. Trypsin solutions with and without *tert*-butylbenzamidinium chloride (∼1 mM) were stored for one week at 7 °C. The solution containing *tert*-butylbenzamidinium and the control were then titrated with benzamidinium chloride. The results were identical within the experimental error, indicating no binding of *tert*-butylbenzamidinium.

For comparison to the ITC results and the free energy calculations, the relative Gibbs energies estimated from octanol/water partition constants[41] of the isolated substituent groups (i.e., going from benzamidinium to *p*-methylbenzamidinium is compared to going from methane to ethane, etc.) are also indicated in Figure 3. Excluding *tert*-butylbenzamidinium, increasing the number of carbons at the first position of the substituent results in a systematic increase in the relative Gibbs energy of binding both experimentally and in the free energy calculations. Increasing the length of the chain initially results in a small rise and then in a slight systematic decrease in the relative Gibbs energy of binding. The absolute magnitude of the changes in Gibbs energy of binding is, however, small when compared to the corresponding estimates from octanol/water partition constants.

Experimentally, the binding constant decreases systematically as the steric bulk at the first carbon of the substituent is increased: $K_{Me} > K_{Et} > K_{i-Pr} > K_{t-Bu}$. One explanation might be that increasing the steric bulk of the substituents leads to a progressive distortion of the binding pocket and its surroundings. However, from Table 2, it is evident that the structure of the backbone of the protein is relatively unaffected. This is also in line with crystallographic studies of trypsin complexes.[11−13] Even *tert*-butylbenzamidinium, which does not bind experimentally, could be accommodated in the structure with no major distortion of the backbone. Interestingly, the larger backbone deviations were observed for complexes of inhibitors with an odd number of carbon atoms in the alkyl chain (methyl, *n*-propyl, *n*-pentyl), although the significance of this is hard to determine, given the small sample size. A rotation of Trp215 (at the beginning of pocket S3/S4) was observed in the

(41) Sangster, J. *Octanol−Water Partition Coefficients: Fundamentals and Physical Chemistry*; Wiley: Chichester, 1997.

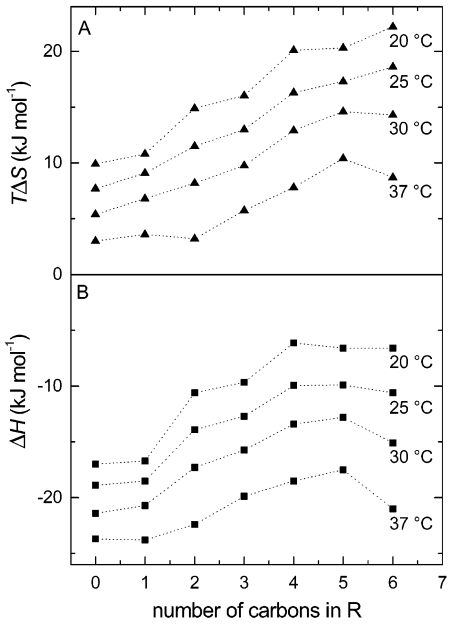

Figure 4. (A) Entropy and (B) enthalpy of binding of *p*-*n*-alkylbenzamidinium chlorides versus the number of carbons in the substituent at 20, 25, 30, and 37 °C in Tris at pH 8.0. Values and errors are listed in Table 1.

simulations of the *p*-*n*-pentylbenzamidinium−trypsin complex, and smaller motions of this group were observed in the *p*-*n*-propylbenzamidinium complex (results not shown). No major systematic distortions in the S1 pocket associated with the elongation of the tail were observed. In the case of the sterically demanding alkyl groups on the para position of the inhibitor, small distortions of the S1 pocket were observed involving Asp189, Ser190, and Gly219 (Table 2). However, as the largest distortion is only 0.18 nm (*n*-propylbenzamidinium), it is doubtful if any are significant.

The binding constant initially falls and then systematically increases upon elongating the chain on the para position: $K_{n-\mathrm{Hex}} > K_{n-\mathrm{Pent}} > K_{n-\mathrm{Bu}} > K_{n-\mathrm{Pr}} > K_{\mathrm{Et}}$. K_{Me} falls between $K_{n-\mathrm{Hex}}$ and $K_{n-\mathrm{Pent}}$, which may be due to this substituent being less sterically demanding. In Figure 4, ΔH and $T\Delta S$ are plotted against the number of carbon atoms in the linear alkyl chain. For all of the compounds except *p*-*n*-hexylbenzamidinium, ΔH becomes less favorable and $T\Delta S$ becomes more favorable upon extending the chain at all temperatures studied. This is characteristic of hydrophobic interactions.[42−45] The behavior of *p*-*n*-hexylbenzamidinium is somewhat different. At low temperatures, there is little to no increase in ΔH on adding an extra methylene group to *p*-*n*-pentylbenzamidinium. At 30 and 37 °C, however, the trend observed for the smaller substituents reverses: adding an extra methylene group to *p*-*n*-pentylbenzamidinium results in a significant decrease in ΔH and an unfavorable change in $T\Delta S$.

In Figure 5, the structure of the binding site of the protein together with the *p*-*n*-butylbenzamidinium ion is illustrated. The alkyl tail of the inhibitor is oriented toward the hydrophobic pocket S3/S4 defined by residues Trp215 and Leu99. Interestingly, when the chain has an odd number of carbons, the terminal methyl group of the tail points away from the pocket.

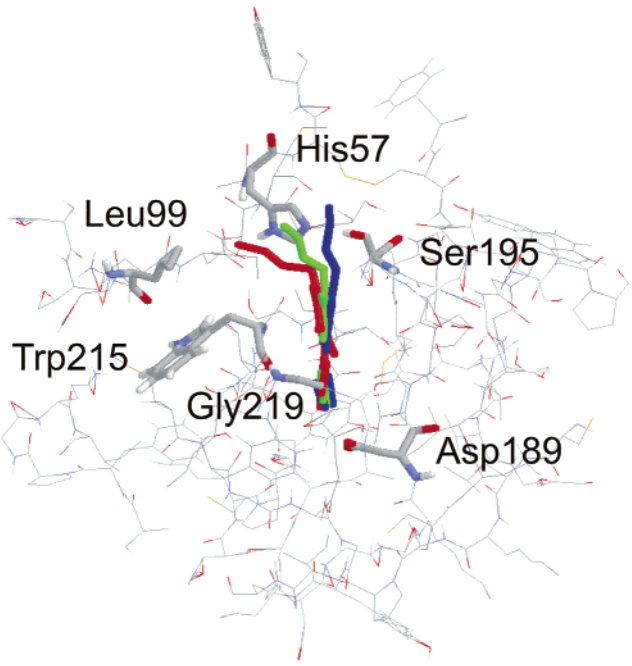

Figure 5. Average structure of the binding site of the *p*-*n*-butylbenzamidinium−trypsin complex at 25 °C. Green, the average structure of the inhibitor; blue and red, configurations illustrating the range of movement of the inhibitor within the binding site. These correspond to the extreme values of the first eigenvector for the motion of the inhibitor obtained from principle component analysis (PCA).

To analyze the dynamics of the system, a principal component analysis (PCA)[46−48] of the motions of the inhibitors inside the S1 pocket was performed. All inhibitors show some motion within the pocket. For the *p*-methyl-, *p*-ethyl-, *p*-*n*-propyl-, *p*-isopropyl-, *p*-*tert*-butyl-, and *p*-*n*-butylbenzamidinium complexes, the average structure corresponds to the most populated conformation. This is illustrated in Figure 5 for the *p*-*n*-butylbenzamidinium complex, which shows the largest motion within this subset of inhibitors. The red and blue structures in Figure 5 correspond to the extremes of the motion. The green structure corresponds to the average (most populated) structure. In contrast, the chains of *p*-*n*-pentyl- and *p*-*n*-hexylbenzamidinium move between two distinct conformations. Figure 6 shows the population distributions at 25 and 37 °C for the *p*-*n*-hexylbenzamidinium complex. The blue and red structures correspond to the predominate conformations at each temperature. The average structure is again green. At 25 °C, the tail is predominately in the S3/S4 pocket. At 37 °C, the two conformations are equally populated. Figure 6C,D shows projections of the first eigenvectors at 25 and 37 °C, respectively. Clearly, the distribution at 37 °C is wider than that at 25 °C. This suggests that the entropy of the bound inhibitor is higher at 37 than at 25 °C. The overall change in entropy on binding is, however, lower at 37 than at 25 °C, reflecting the fact that the entropy is dominated by the displaced solvent and not by the bound inhibitor.

(42) Lee, B. *Biophys. Chem*. **1994**, *51*, 271−278.
(43) Blokzijl, W.; Engberts, J. B. F. N. *Angew. Chem., Int. Ed. Engl.* **1993**, *32*, 1545−1579.
(44) Graziano, G. *Phys. Chem. Chem. Phys* **1999**, *1*, 3567−3576.
(45) Southall, N. T.; Dill, K. A.; Haymet, A. D. J. *J. Phys. Chem. B* **2002**, *106*, 2812.
(46) Karplus, M.; Kushick, J. N. *Macromolecules* **1981**, *14*, 325−332.
(47) García, A. E. *Phys. Rev. Lett.* **1992**, *68*, 2696−2699.
(48) Amedei, A.; Linssen, A. B. M.; Berendsen, H. J. C. *Struct., Funct. Gen.* **1993**, *17*, 412−425.

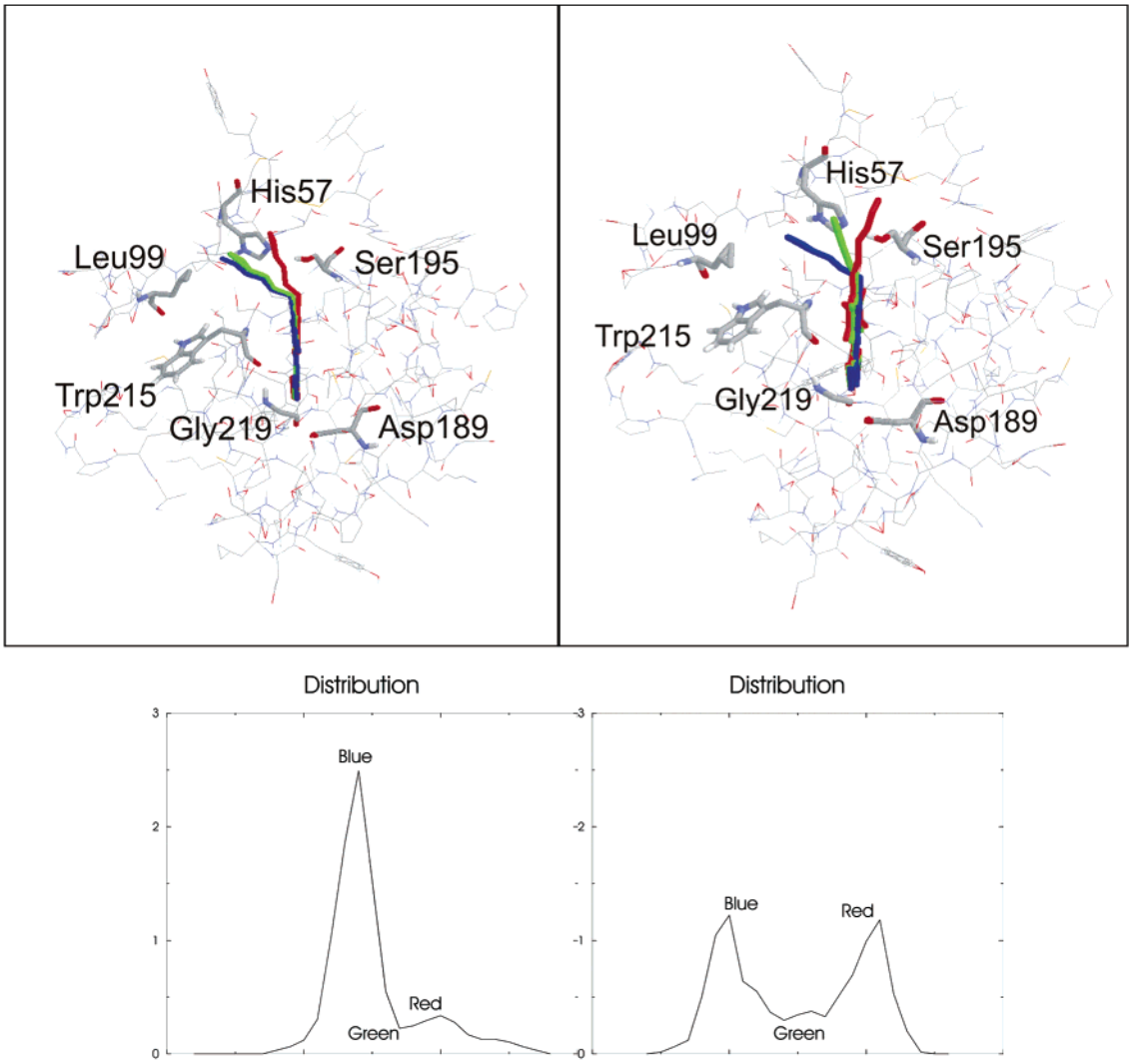

Figure 6. (Upper plots) The average structure of the binding site of the *p*-*n*-hexylbenzamidinium−trypsin complex at (left, A) 25 and (right, B) 37 °C. Green, the average structure of the inhibitor; blue and red, configurations corresponding to the values of the first eigenvector with maximum probability. (Lower plots) Graphs showing the distribution along the first eigenvector obtained from a PCA of the motion of the inhibitor within the binding site at (left, C) 25 and (right, D) 37 °C.

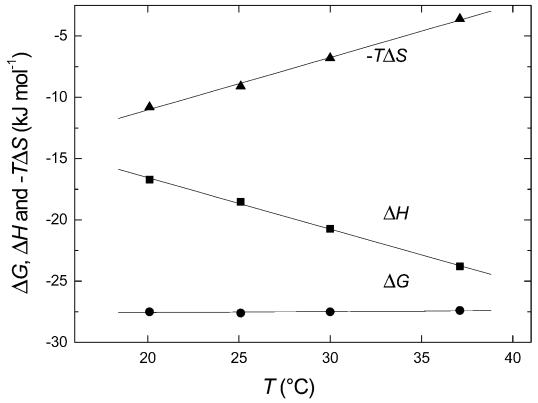

Figure 7. Δ*G*, Δ*H*, and −*T*Δ*S* of binding of *p*-methylbenzamidinium chloride at 20, 25, 30, and 37 °C in Tris at pH 8.0. Values and errors are listed in Table 1.

Heat Capacity Change upon Binding. The hydrophobic properties of the inhibitors can also be inferred from the temperature dependence of the thermodynamic parameters. Figure 7 depicts the temperature dependence of Δ*G*, Δ*H*, and *T*Δ*S* of the binding of *p*-methylbenzamidinium chloride to trypsin. ΔC_p, the heat capacity change upon binding, is given by

$$\partial \Delta H / \partial T = \Delta C_p \qquad (4)$$

From Figure 7, it is clear that, in the temperature range studied, Δ*H* is linearly dependent on *T*. This is also true for the other *p*-alkylbenzamidinium chlorides. For each inhibitor, ΔC_p was estimated from the slope of a least-squares line of the best fit to the Δ*H* data. The results are listed in Table 4.

Figure 8 shows the dependence of ΔC_p on the number of carbon atoms in the linear alkyl chain. Overall, ΔC_p becomes more negative with increasing chain length. Interestingly, inhibitors with an odd number of carbon atoms in R have a less negative (or those with an even number have a more negative) ΔC_p than expected, leading to a zigzag pattern. A similar pattern is evident in the simulations. Odd-numbered chains show slightly larger RMS backbone positional deviations (Table 2) and have the terminal carbons projecting away from the protein. However, this is not reflected in the change in solvent-accessible surface area of the inhibitor on binding (see below).

Table 4. ΔC_p, T_S and T_H, and the Solvent-Accessible Surface[a] of the Inhibitor before (SAS(aq.)) and after (SAS(tryps.)) Binding, for Binding of *p*-Alkylbenzamidinium Chlorides to Trypsin[b]

R[c]	ΔC_p (J mol^{-1} K^{-1})	T_s (°C)	T_H (°C)	SAS(tryps.) (nm^2)	SAS(aq.) (nm^2)
H[d]	−400 ± 20	44	−23	0.40	2.78
Me[d]	−420 ± 12	46	−19	0.35	2.83
Et[e]	−693 ± 12	42	4.8	0.48	3.19
n-Pr	−598 ± 2	47	3.9	0.68	3.46
i-Pr[e]	−419 ± 4	63	8.4	0.36	3.37
n-Bu	−728 ± 4	48	12	0.87	3.70
n-Pent	−632 ± 10	55	9.6	0.87	3.90
n-Hex	−849 ± 10	48	12	0.92	4.15

[a] The solvent-accessible surface was computed numerically[49] on the basis of an average structure. The atomic radii used were 0.16 nm for carbon, 0.13 nm for oxygen, 0.14 nm for nitrogen, 0.20 nm for sulfur, and 0.10 nm for hydrogen atoms. The atomic radius of the solvent was 0.14 nm. [b] Titrations performed in 50 mM Tris, 10 mM $CaCl_2$ buffer at pH 8.0. [c] Substituent at para position. [d] Data taken from ref 15. [e] Since these compounds contain some NH_4Cl, control experiments were performed with 10 wt % NH_4Cl added to a benzamidinium chloride solution at the usual concentration. Within error, the thermodynamic parameters were identical. Therefore, the concentrations of these inhibitors, based on weight, can be safely corrected for the amount of NH_4Cl present.

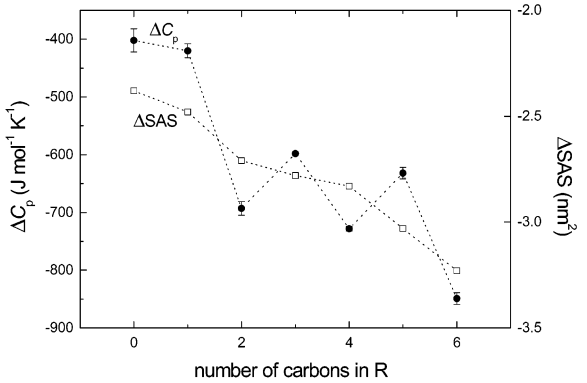

Figure 8. Heat capacity change (ΔC_p, *y*-axis left-hand side) and change in the solvent accessible surface (ΔSAS, *y*-axis right-hand side) upon binding of *p*-*n*-alkylbenzamidinium ions to trypsin versus the number of carbons in the substituent in Tris at pH 8.0. Values and errors are listed in Table 4.

Thermodynamic data from various sources, i.e., the transfer of compounds from a nonpolar phase to water,[50,51] protein folding,[50−52] and the binding of different ligands to proteins,[52−54] suggest that a negative value of ΔC_p often correlates with the burial of nonpolar (hydrophobic) surface area. The burial of a polar surface results in an increase of ΔC_p. Although the precise origin of this hydrophobic effect is still debated, a common interpretation is that hydrophobic surfaces induce the tangential orientation (relative to the surface) of the water O−H bonds in the first hydration shell[42−45,55] and that this ordered water is released on burial of the surface.

The marked decrease in ΔC_p with increasing chain length suggests that the burial of a hydrophobic surface is a major factor in binding. In Table 4, the values of the solvent-accessible surface of the inhibitor calculated free in solution (SAS(aq.)) and bound to the protein (SAS(tryps.)) are given. The net change in the solvent-accessible surface area of the inhibitor on binding is plotted in Figure 8. For the longer alkyl tails (*n*-Pent and *n*-Hex), there is little or no change in SAS(tryps.) (Table 4). This suggests that the longer alkyl tails are partially buried (presumably in the S3/S4 groove) and not exposed to water.

A negative ΔC_p means that the net thermodynamic driving force for association will shift from being entropic to enthalpic with increasing temperature. Temperatures T_S and T_H can be defined, at which the entropic and the enthalpic contributions to binding are zero. T_S and T_H were calculated from a linear fit to the temperature dependence of $T\Delta S$ and ΔH and are listed in Table 4.

From Figure 7, it can be seen that ΔG is practically independent of temperature. This is a result of a compensation between ΔH and $T\Delta S$, which are both linearly dependent on temperature. Such behavior is characteristic of processes with a large, negative ΔC_p[42,44,45,55] and is a consequence of the vanishing of the hydrophobic hydration of the inhibitor. This enthalpy−entropy compensation arises from the relative magnitudes of ΔS and ΔC_p.[42,54] The change in the enthalpy and the entropy upon variation of the temperature are given respectively by eq 4 and the following:

$$\partial T\Delta S/\partial T = \Delta C_p + \Delta S \tag{5}$$

When $|\Delta C_p| \gg |\Delta S|$ at all temperatures, the temperature dependence of ΔS is approximately equal to ΔC_p. This means that the temperature dependences of both ΔH and ΔS are equal to ΔC_p, which results in ΔG being relatively temperature-independent. The enthalpy−entropy compensation is similar for almost all of the *p*-alkylbenzamidinium chlorides studied. Only in the case of the *n*-pentyl and *n*-hexyl substituents was complete compensation not observed. In these cases, $\delta\Delta H/\delta T$ has a larger negative value than $\delta T\Delta S/\delta T$ and leads to a decrease in ΔG upon increasing temperature. This could be due to the tail being more dynamic at higher temperatures (Figure 6), which results in the overall entropy change upon binding being more favorable at higher temperatures than expected.

Dehydration of the Active Site. The binding of several natural inhibitors is known to induce an acidic shift in the pK_a of His57 N2.[56,57] This pK_a shift is attributed to the cost of burying a charged His57 in an apolar environment, which is only partly compensated by a stronger Ser195−His57 hydrogen bond in the complex.[56,57] To examine whether a change in the protonation state of His57 N2 also occurs upon binding of the benzamidinium-based inhibitors to trypsin, we investigated the dependence of binding of benzamidinium chloride and *p*-*n*-hexylbenzamidinium chloride on the buffer used. When protonation/deprotonation effects are coupled to binding, ΔH depends not only on the intrinsic enthalpy of binding ΔH_{int} but also on the enthalpy change associated with the ionization of the buffer.[17,18] This can be expressed as

$$\Delta H = \Delta H_{int} + N_{H^+}\Delta H_{ion} \tag{6}$$

where N_{H^+} is the number of protons from the buffer taken up by the enzyme and ΔH_{ion} is the ionization enthalpy of the buffer. N_{H^+} is equal to the change in the protonation state of residues

(49) Eisenhaber, F.; Lijnzaad, P.; Argos, P.; Sander, C.; Scharf, M. *J. Comput. Chem.* **1995**, *16*, 273−284.
(50) Spolar, R. S.; Livingstone, J. R.; Record, M. T. *Biochemistry* **1992**, *31*, 3947−3955.
(51) Murphy, K. P.; Privalov, P. L.; Gill, S. J. *Science* **1990**, *247*, 559−561.
(52) Sturtevant, J. M. *Proc. Natl. Acad. Sci. U.S.A.* **1977**, *74*, 2236−2240.
(53) Spolar, R. S.; Record, M. T. *Science* **1994**, *263*, 777−784.
(54) Ha, J. H.; Spolar, R. S.; Record, M. T. *J. Mol. Biol.* **1989**, *209*, 801−816.
(55) Sharp, K. A.; Madan, B. *J. Phys. Chem. B* **1997**, *101*, 4343−4348.
(56) Baker, B. M.; Murphy, K. P. *J. Mol. Biol.* **1997**, *268*, 557−569.
(57) Antonini, E.; Ascenzi, P.; Bolognesi, M.; Gatti, G.; Guarneri, M.; Menegatti, E. *J. Mol. Biol.* **1983**, *165*, 543−558.

Table 5. Thermodynamic Parameters for Binding of *p*-Alkylbenzamidinium Chlorides to Trypsin at 25 °C[a]

R[b] (pH)	buffer	K (10^4 M^{-1})	ΔG (kJ mol^{-1})	ΔH (kJ mol^{-1})	$T\Delta S$ (kJ mol^{-1})
H (8.0)	Hepes	5.3 ± 0.3	-26.9 ± 0.1	-17.9 ± 0.1	9.0 ± 0.2
	Bicine	6.3 ± 0.1	-27.4 ± 0.1	-16.0 ± 0.8	11.4 ± 0.9
	Tricine	4.6 ± 0.4	-26.6 ± 0.2	-16.8 ± 0.5	9.8 ± 0.6
	Glycylglycine	5.0 ± 0.4	-26.8 ± 0.2	-16.5 ± 0.2	10.3 ± 0.3
	Tris	4.5 ± 0.2	-26.6 ± 0.1	-18.9 ± 0.4	7.7 ± 0.5
H (7.4)	Pipes	4.6 ± 0.2	-26.6 ± 0.1	-13.2 ± 0.3	13.4 ± 0.4
	Hepes	4.9 ± 0.3	-26.8 ± 0.2	-15.3 ± 0.4	11.5 ± 0.5
	Bicine	4.3 ± 0.3	-26.5 ± 0.2	-15.7 ± 0.6	10.8 ± 0.6
	Tricine	3.8 ± 0.3	-26.1 ± 0.2	-16.5 ± 0.8	9.6 ± 0.9
n-Hex (7.4)	Pipes	15 ± 1	-29.5 ± 0.2	-2.9 ± 0.2	26.6 ± 0.4
	Hepes	14 ± 1	-29.4 ± 0.2	-6.2 ± 0.3	23.2 ± 0.6
	Bicine	13 ± 1	-29.2 ± 0.2	-6.6 ± 0.3	22.6 ± 0.5
	Trycine	12 ± 1	-29.1 ± 0.2	-8.4 ± 0.4	20.7 ± 0.3

[a] Titrations performed in 50 mM concentrations of the different buffers (10 mM $CaCl_2$) at pH 8.0 or 7.4. [b] Substituent at the para position.

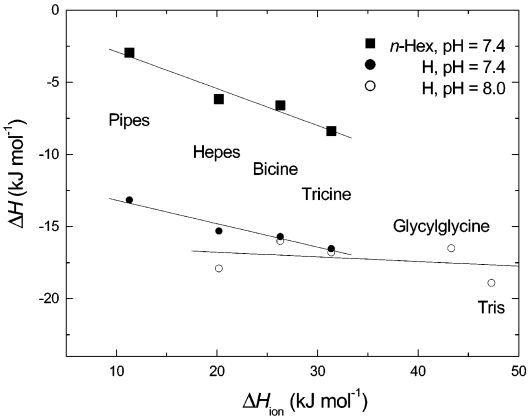

Figure 9. Enthalpy of binding of benzamidinium chloride at pH 8.0 and 7.4 and of *p*-*n*-hexylbenzamidinium chloride at pH 7.4 versus the ionization enthalpy[58] of the buffer. See Table 5.

involved in the binding process. At a given pH, the change in the fraction of protonated His57 N2 can be calculated by using the Henderson−Hasselbalch equation:

$$\mathrm{pH} = \mathrm{p}K_a + \log \frac{[\mathrm{His57}]}{[\mathrm{His57^+}]} \qquad (7)$$

where [His57] is the concentration of unprotonated His57 N2 and [His57$^+$] is the concentration of protonated His57 N2.

Table 5 lists the thermodynamic parameters of binding of benzamidinium chloride to trypsin at 25 °C in several buffers at pH 8.0 and of benzamidinium chloride and *p*-*n*-hexylbenzamidinium chloride at pH 7.4. Figure 9 shows the dependence of the enthalpy of binding on the ionization enthalpy of the buffer for benzamidinium chloride at pH 8.0 and 7.4 and for *p*-*n*-hexylbenzamidinium chloride at pH 7.4, both at 25 °C. For benzamidinium chloride at pH 8.0, the linear regression yields an abscissa, equal to ΔH_{int}, of $-16.3(1.9)$ kJ mol^{-1} and a slope, equal to N_{H^+}, of $-0.03(0.05)$ indicating that, within error, no protons are transferred upon binding. By contrast, for benzamidinium chloride at pH 7.4, the values of ΔH_{int} and N_{H^+} are $-11.6(0.61)$ kJ mol^{-1} and $-0.16(0.03)$, respectively. Thus, at pH 7.4, protons are transferred upon binding, and the binding constant decreases due to a less favorable ΔH_{int} that is partly compensated by a more favorable entropic contribution.

It is interesting to look at the influence of an alkyl chain at the para position on the thermodynamics of binding and N_{H^+}.

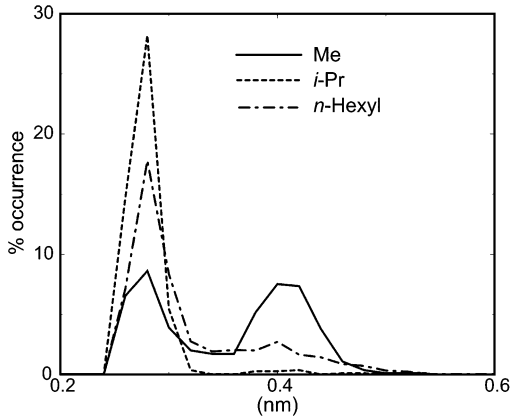

Figure 10. Distribution functions of the distance (nanometers) between the oxygen OG of Ser195 and the nitrogen N2 of His57 in the complexes of trypsin with *p*-methyl-, *p*-isopropyl-, and *p*-*n*-hexylbenzamidinium ions.

For *p*-*n*-hexylbenzamidinium chloride at pH 7.4, the values of ΔH_{int} and N_{H^+} are $-0.3(0.96)$ kJ mol^{-1} and $-0.26(0.04)$, respectively. Since at pH 7.4 the intrinsic enthalpy of binding is close to zero, the driving force for binding is almost entirely entropic. It is evident that more protons are transferred upon binding for *p*-*n*-hexylbenzamidinium chloride than for benzamidinium chloride. Using eq 7, the change in the fraction of protonated His57 N2 for a serine proteinase upon binding of a protein inhibitor at pH 7.4 was estimated to be -0.28.[59] This decrease in the fraction of protonated His57 N2 corresponds to a transfer of -0.28 proton from the buffer to the enzyme (N_{H^+}).[60] This is (within error) equal to that reported for the binding of *p*-*n*-hexylbenzamidinium chloride to trypsin and larger than that reported for benzamidinium chloride (see above). Since the decrease of the fraction of protonated His57 reflects a dehydration penalty, these data indicate that His57 is more shielded from water upon binding of *p*-*n*-hexylbenzamidinium chloride than upon binding of benzamidinium chloride.

To understand the origin of this pK_a shift, the average number of water molecules in the active site around the OG of Ser195 and the N2 of His57 in the simulations was examined. Upon increasing the number of carbon atoms in the *p*-alkyl substituent, the two residues (in particular His57) become progressively less accessible to water. The more sterically demanding substituents shield the active site from water (results not shown). For these inhibitors, the penalty for dehydration of the active site on binding will be larger. Exclusion of water from the active side promotes the formation of a hydrogen bond between the OG of Ser195 and the N2 of His57. Figure 10 shows the distribution of this distance between the OG of Ser195 and the N2 of His57 for the complexes of trypsin with methyl-, isopropyl-, and *n*-hexylbenzamidinium ions. The distributions have two maxima: one at 2.8 Å (a H-bonding distance) and the other around 4.0 Å. In general, the larger the substituent, the more probable is a hydrogen bond between the two residues.

(58) Christensen, J. J.; Hansen, L. D.; Izatt, R. M. *Handbook of Proton Ionization Heats and Related Thermodynamic Quantities*; Wiley: New York, 1976.
(59) At pH 7.4, the fraction of protonated His57 N2 amounts to 0.285 for pK_a = 7 and 0.004 for pK_a = 5.
(60) Baker and Murphy[56] report a pK_a shift of His57 from 6.7 in the free elastase to 5.2 in the ovomucoid third domain−elastase complex. Using their data at pH 7, an experimental value of around -0.29 for N_{H^+} is found, while a calculated value of -0.32 is found using the Henderson−Hasselbalch equation, indicating that this approach leads to good agreement with experiment.

As the substituent binds into the hydrophobic pocket S3/S4, one might expect that binding would strongly correlate with octanol/water partition constants.[41] From Figure 3 it is clear this is not the case. The fact that inhibitor binding is associated with the dehydration of the active site, the pK_a shift of His57, and the changes in the interaction between Ser195 and His57 goes some way to explain this apparent discrepancy. The effect of dehydration of the protein should, however, be reflected in the free energy calculations. The GROMOS96 force field accurately reproduces the cyclohexane/water partition properties of small linear and branched aliphatic compounds.[38] However, the force field is known to underestimate the Gibbs energy of hydration of analogues of the more polar α-amino acids, including Trp. Thus, we would expect the calculations to correctly reproduce the hydrophobic contributions to binding but to underestimate the cost of dehydration of the protein, leading to an overestimation of the experimental binding Gibbs energies, as is seen. Thus, the free energy calculations reinforce the idea that dehydration is an important determining factor for binding. Note that the degree of dehydration of the catalytic triad is influenced by both the length of the substituent and the degree of branching at the first carbon (Figure 10). Thus, for the ethyl and isopropyl substituents, for example, one cannot distinguish steric effects due to clashes with the protein from the increased dehydration of the active site.

Conclusions

Understanding molecular recognition requires knowledge of the thermodynamic properties of the system, together with insight into the structure and dynamics of the complex of interest. Here, ITC experiments and MD simulations have been used to study the binding of a series of *p*-alkylbenzamidinium chloride inhibitors to trypsin, to understand the influence of small structural variations in the alkyl substituent on binding.

The steric and hydrophobic properties of the *p*-alkyl substituent are clearly correlated with binding affinity. Steric bulk on the first carbon decreases the binding affinity. Experimentally, the binding of *p-tert*-butylbenzamidinium was found to be negligible. The presence of a hydrophobic linear alkyl tail increases the binding affinity. Increasing the length of the *p-n*-alkyl tail ($n = 2-6$) resulted in a progressive (favorable) increase in the entropy of binding. This was partially compensated by an unfavorable increase in the enthalpy of binding. The change in heat capacity upon binding becomes more negative with increasing tail length, suggesting that binding is dominated by hydrophobic interactions.

However, the above picture is overly simplistic. Simulation studies suggest that all of the inhibitors, including *p-tert*-butylbenzamidinium, can be accommodated within the binding pocket without obvious strain. Free energy calculations predict that the binding of *p-tert*-butylbenzamidinium is favorable, suggesting that the failure of *p-tert*-butylbenzamidinium to bind may be due to an inability to enter the binding pocket rather than steric restrictions. Comparison with octanol/water partition data also suggests that the changes in binding Gibbs energy on extending the chain length of the substituent are small compared to that expected for a purely hydrophobic interaction. In fact, the binding constants for these inhibitors are remarkably similar, indicating that there is a penalty for binding which must be considered. Calculation of the pK_a shift of His57 shows that the alkyl substituents shield the active site from water. The larger and more sterically demanding a substituent is, the less water can be found around Ser195 OG and His57 N2. This dehydration, which mechanistically is associated with the activation of the catalytic triad, also incurs a thermodynamic cost and results in a lower affinity.

Overall, the study shows that, even in the case of a simple series of substituents, the factors that determine the binding affinity can be highly involved. Superficially, the series of compounds investigated display only small differences in binding affinity (except for *p-tert*-butylbenzamidinium, which does not bind). Detailed thermodynamic analysis showed, however, that this masks large compensating differences in enthalpy and entropy. Simulation studies in turn showed that simple concepts such as steric hindrance and hydrophobic interactions based on buried surface area were insufficient to fully explain the results. Secondary effects, such as an ability to access the binding site and the cost of dehydration of the active site, are of equal or even greater importance. The present study serves to underline the danger of using empirical models based on the structural properties of an inhibitor alone to rationalize binding behavior, even in the simplest cases.

Acknowledgment. Thorsten Stafforst is gratefully acknowledged for synthesizing *p*-ethylbenzamidinium chloride.

Supporting Information Available: Synthesis and analysis of *p*-alkylbenzamidinium chlorides (PDF). This material is available free of charge via the Internet at http://pubs.acs.org.

JA034676G